Effect of External Electric Field on Morphologies and Properties of the Cured Epoxy and Epoxy/Acrylate Systems

Jingkuan Duan,[1,2] Jun Zhang,[2] Pingkai Jiang[2]

[1]*Institute of Material Engineering of Ningbo University of Technology, Ningbo, People's Republic of China*
[2]*Shanghai Key Laboratory of Electrical Insulation and Thermal Aging, School of Chemistry and Chemical Engineering, Shanghai Jiaotong University, Shanghai, People's Republic of China*

Received 3 June 2010; accepted 8 September 2010
DOI 10.1002/app.33368
Published online 29 December 2011 in Wiley Online Library (wileyonlinelibrary.com).

ABSTRACT: In this article, the influences of the external electric field exerted to the curing epoxy and epoxy/acrylate systems on their cured microstructures and macroscopic performances were investigated by means of morphological investigation and some characteristic analyses. Epoxy and epoxy/acrylate (an interpenetrating polymer network) systems were subjected to the action of the alternating electric field during the curing process. The changes in the nanolamellae microstructure in the cured epoxy and the nanoellipsoid microstructure in the cured epoxy/acrylate systems resulting from the electric field treatment were observed using atomic force microscopy. Dynamic mechanical analysis showed that the external electric field treatment made the low and high relaxation peaks shift to the lower and higher temperatures, respectively. Thermogravimetric analysis implied that the curing reactions of the epoxy systems with the aid of the external electric field resulted in some negative influences on their thermal stability. The dielectric measurements demonstrated that the electrical properties of the epoxy system for vacuum pressure impregnation insulation of the high-voltage electric machines could be much improved with the aid of the external electric field. © 2011 Wiley Periodicals, Inc. J Appl Polym Sci 125: 902–914, 2012

Key words: epoxy; cure reaction; electric field treatment; morphology; dielectric property

INTRODUCTION

Epoxy resins as the main insulating materials are widely used in high-voltage electrical applications, and the demand of further improving its performances is necessarily increasing with the rapid development of the electrical and electronic industries. Therefore, much effort has been given to the research on how to improve the electrical, mechanical, thermal, and physicochemical properties of the cured epoxy resin systems.

As well known, electric, magnetic, and electromagnetic fields can be effectively used for modifying the properties and morphologies of the polymeric materials and their composites. In some kinds of the single polymeric materials, multifunctional properties can be obtained by other technologies such as self-assembly and field-aided microtailoring by which the local optimization of microstructure in polymeric material can be obtained.[1,2] Field-aided microtailoring technology is an approach in which the external field, such as electric, magnetic, or mechanical field, is used to modify the structure of liquid or melt polymeric materials, and it makes the resulting polymeric materials own locally microtailored aligned or orientated structures.[3]

It is well known that the physical properties of the polymers strongly depend on their microstructures. The ongoing quest for designing novel molecular materials, understanding their intrinsical properties, and improving their performance in real devices, therefore, requires control fully over their spatial arrangement. The molecular alignment and orientation have attracted great interest for a long time in physics and chemistry because of their importance to fundamental research and technology applications.[4,5]

There are many methods to achieve uniform orientation or alignment in polymeric materials, such as mechanical, magnetic, and electric fields. To achieve large-scale alignment throughout a macroscopically extended bulk sample, most prominently, external mechanical fields have been successfully applied to orient some polymers.[6–9] However, these technologies susceptibly lead to an inhomogeneous microstructure observable as a characteristic striped pattern of the direction orientation.[10] In addition, they are not applicable to thin films.

Correspondence to: P. Jiang (pkjiang@sjtu.edu.cn).
Contract grant sponsor: Shanghai Committee of Science Technology funds for Major Research Project of Shanghai City; contract grant number: 05dz22303.

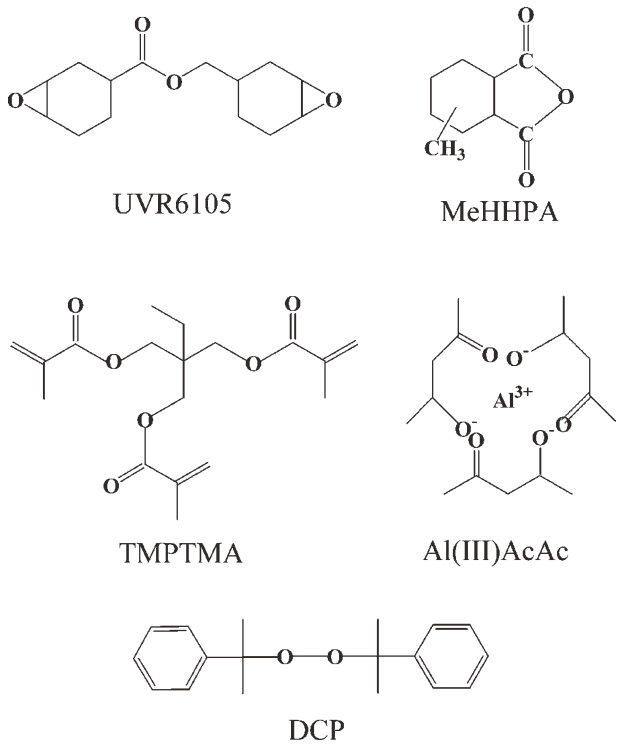

Figure 1 Chemical structures of the cycloaliphatic epoxy resin, UVR6105; the curing agent, MeHHPA; the modifier, TMPTMA, the latent accelerator, Al(III)AcAc; and initiator, DCP.

Magnetic field is another effective method to obtain alignment or orientation in polymers, which is applied only to the material having large magnetic susceptibility anisotropy.[11,12]

Recently, the potential of electric field application for microdomain alignment is attracting increasing interest because it may also have a considerable technological possibility and benefit.[13–17] The application of the electric field to fluids has been explored in a number of systems, including molecular liquids, ferrofluids, electrorheological fluids, materials that exhibit liquid crystalline phase showing the dielectric anisotropy on a molecular scale, and the block copolymers.[18–23]

Some thermosets such as liquid crystalline epoxides can offer the possibility of producing bulk layered structures with macroscopic orientation if their curing reaction proceeds in an aligning field. However, little studies on orientation or alignment behaviors of cycloaliphatic epoxy resin (CER), which owns a relatively regular structure, and its composites, e.g., CER/acrylate system, has been reported up to now.

The objective of this work was to investigate the effects of the external electric field on the morphological, chemical, physical, and thermal properties of a single network system (the anhydride-CER system) and an interpenetrating polymer networks (IPNs) system composed of CER and acrylate.

EXPERIMENTAL

Materials

A difunctional CER (marketed under the trade designation UVR6105) was purchased from Dow Chemical Company, Midland, MI. The epoxy equivalent weight was 126–135 g/mol. The curing agent was methyl-hexahydrophthalic anhydride (marketed under the trade designation LHY-807), obtained from Shanghai Li Yi Science and Technology Development Co., China. The molecular weight was 168.19 g/mol. The latent accelerator used was aluminum(III) acetylacetonate (Al(III)AcAc), purchased from Aldrich Chemical Co. (St. Louis, MO). Trimethylol-1,1,1-propane trimethacrylate (TMPTMA) was obtained from Jinshi Tech-Development Co., China. The viscosity of TMPTMA was 30–60 mPa s (25°C). The dicumyl peroxide (DCP) initiator was purchased from Aldrich Chemical Co. The chemical structures of the raw materials are shown in Figure 1.

Experimental setup

The curing setup is depicted in Figure 2. The external electric field was applied between an upper electrode amounted on the upper insulating plate (glass) and the metal container. The electric field intensity E at the interelectrode space of 3.3 mm (the sum of the sample and the air layer thickness) was kept constant as $E = 1.2$ kV/mm. The total weight of the liquid sample taken for the curing reaction was around 6,537,412 g, and then each sample was cured at 160°C for 10 h using this setup placed in a closed clamber.

Samples preparation

All the liquid raw materials were purified before mixing with one another to afford the excellent and uniform properties to the cured samples. The epoxy resin, curing agent, and modifier agent were degassed in vacuum at 80°C for 30 min. The latent accelerator and initiator were used without any further purification. The epoxy resin and latent

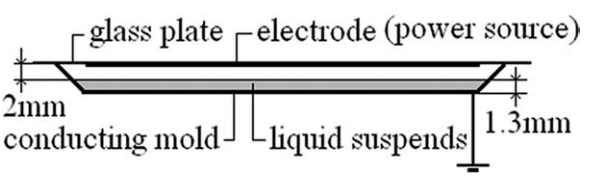

Figure 2 Scheme of setup for curing of CER and CER/TMPTMA systems with the aid of the electric field.

TABLE I
The Formation and Conditions of Experiment

Sample	CER system	CER/TMPTMA system
6105, pbw	100	100
MeHHPA, pbw	95	95
Al(III)AcAc, pbw	0.4	0.4
TMPTMA, pbw	0	30
DCP, pbw	0	0.03
Curing conditions	AC E = 1.2 kV/mm; frequency = 50 Hz	

pbw, parts by weight.

accelerator were weighed in proper equivalences and mixed vigorously with each other at 120°C until the latent accelerator was completely dissolved. Then, the blends of epoxy resin and accelerator were rapidly cooled down to the ambient temperature, and the curing agent, modifier agent, and initiator were added in suitable amounts according to the composition given in Table I, and mixed for about 10 min to give the homogeneous liquid blends.

The liquid compounds were added into the setup as shown in Figure 2. The conducting stainless steel mold was maintained electrically at the ground potential, and a copper-coated glass plate, where the circular copper-coated part is electrically at the high potential, covered the conductive mold containing the liquid mixture. The curing reaction was carried out in this air-tight setup placed in an oven. The cured pellets were cut relatively sharp to measure the different properties.

Characterizations and measurements

Atomic force microscopy

For atomic force microscopy (AFM) observation, the specimens cured with and without the aid of the external electric field were trimmed using a Leica Ultracut UCT ultramicrotome either parallel or perpendicular to the direction of the applied electric field, and the thickness of the specimens was about 70 nm. The morphological observation of the samples was conducted on a Nanoscope IIIa scanning probe microscope (Digital Instruments, Santa Barbara, CA) in a tapping mode.

Fourier transform infrared spectroscopy

Fourier transform infrared spectroscopy (FTIR) reflection measurement was performed by means of a Paragon 1000 (Perkin–Elmer, Waltham, MA) with a resolution of 4 cm^{-1}.

Wide-angle X-ray diffraction

X-ray diffraction measurements were performed using a D/max-2200/PC X-ray diffractometer with CuK_α radiation (Rigaku Corp., Japan; $\lambda = 1.5405$ Å). Diffraction spectra were obtained in a 2θ range of 1–60°, and the diffraction angle was scanned at a rate of 2° min^{-1}.

Dynamic mechanical analysis

The tangent delta of the cured samples was measured with TA 2980 dynamic mechanical analyzer by using single cantilever mode. The geometry of specimens is 25 mm × 5.0 mm × 1.3 mm (length × width × thickness). Scans were conducted in a temperature range of 50–250°C at a heating rate of 3°C/min and a frequency of 1 Hz.

Thermogravimetric analysis

Thermogravimetric analysis (TGA) was performed using a Cahn TG systems 41 thermogravimetric analyzer. Samples were heated up to 800°C from the ambient temperature at the heating rate of 5°C/min under air atmosphere.

Dielectric measurements

The dielectric breakdown tests of the cured samples were performed at the room temperature using 50-Hz, 100-kV high-voltage transformer (Shanghai Lanpo High Voltage Technology and Equipment Co., Shanghai, China). The cured samples were inserted between two spherical electrodes with the radii of 10 mm, and then the measuring electrode system containing the measuring specimen was immersed in a tank filled with silicon oil so as to prohibit the flashover along the surface of the specimen. During testing, the applied voltage was raised step by step (the voltage ratio between adjacent steps is 2),[24] and the voltage at each step was kept for 1 min. The initial test voltage was 20 kV and the rate-of-rise of the test voltage is 2 kV/min.

Dielectric responses were measured using a CONCEPT 40 brand frequency impedance analyzer (NOVOCONTROL, Hundsangen, Germany) in the comparatively wide frequency range of 1 kHz to 10 MHz and at room temperature.

RESULTS AND DISCUSSION

Curing mechanisms of the CER and CER/TMPTMA systems

For the sake of elucidating the influences of the application of the external electric field during the curing reaction on the network formation and the morphological structures of the cured epoxy systems studied, it is necessary to understand the curing reaction mechanisms of the CER and CER/TMPTMA system.

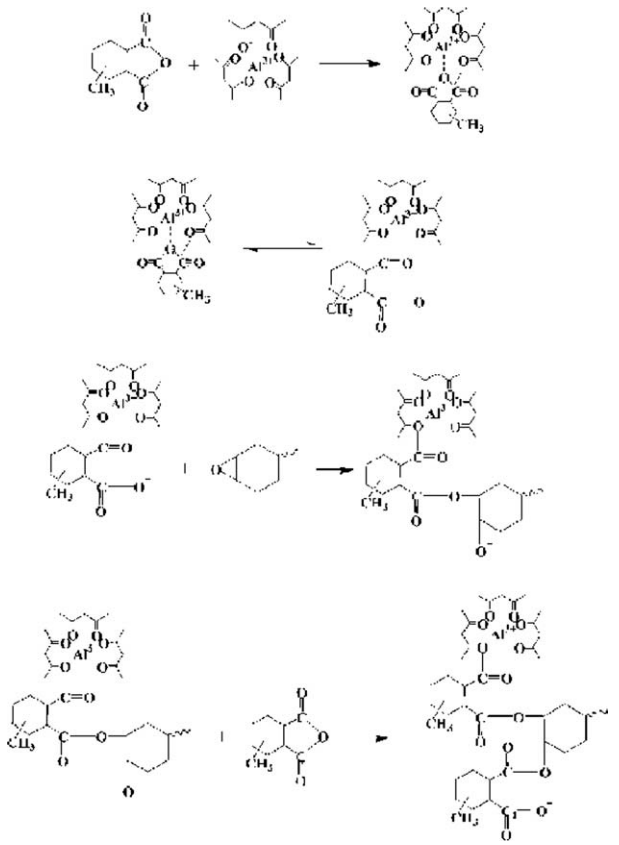

Figure 3 The schematic reactions between epoxy and anhydride accelerated by aluminum acetylacetonate.

In the CER system, there exists a polyaddition reaction during the thermal curing, the mechanism of which is more complicated owing to the catalytic action of the aluminum acetylacetonate. Many researchers have studied the catalytic behaviors of metal acetylacetionates for the epoxy curing reactions.[25,26] Figure 3 depicts the possible schematic reaction between epoxy and anhydride, accelerated by aluminum acetylacetonate.

In this case, a metal chelate with the first-row transition metal ions is possibly yielded by Al(III)AcAc when the systems are heated, and the anhydride thermally disassociates into super acids because of the catalysis of the metal chelates as shown in Figure 3. The super acids attack the oxirane rings fused to a cyclohexyl ring in the epoxy resin to initiate the opening of the oxirane rings, which, in turn, results in the presence of many dipoles in the system during the curing reaction. Some dipoles present in the anhydride-CER system take part in the polyaddition reactions, and some new types of dipoles are newly formed. These reactions play an important role in the chain extension, branching, and cross-linking of the molecules resulting from the reaction, which finally leads to the formation of the three-dimensional network.

In the CER/TMPTMA system, there exist two kinds of the curing reactions to proceed sequentially during the formation of IPNs consisting of both TMPTMA and CER networks, that is, the free-radical polymerization of TMPTMA and the thermal polyaddition of the epoxy resin.

One should keep in mind that the polymerization of TMPTMA monomers is likely independent of the polyaddition reaction between the epoxy resin and the hardener. Owing to the much shorter half-life of DCP, the free-radical polymerization of TMPTMA is prior to the polyaddition of the anhydride-CER system, which leads to a sharp enhancement of the viscosity in the system before the occurrence of the CER curing. The much higher viscosity would be an obstacle to the mobility of epoxy molecules. As the curing reaction proceeds, the curing reaction of the CER system just begins to occur in the presence of the network of TMPTMA as the reacting course. The possible schematic reaction between TMPTMA and DCP is given in Figure 4.

From Figures 3 and 4, it is found that there exist large amount of induced and permanent dipoles in the CER and CER/TMPTMA systems during their curing reaction. The molecules containing permanent dipole moments in the systems are subjected to external fields during cure stage, and because of the induced polarization, an orientation torque exists. This torque that causes the alignment is proportional to the square of the applied field when the electric field is relatively small. Therefore, even if no permanent dipole moment is considered, the charged macromolecules formed during cure should rotate to align with the external field.

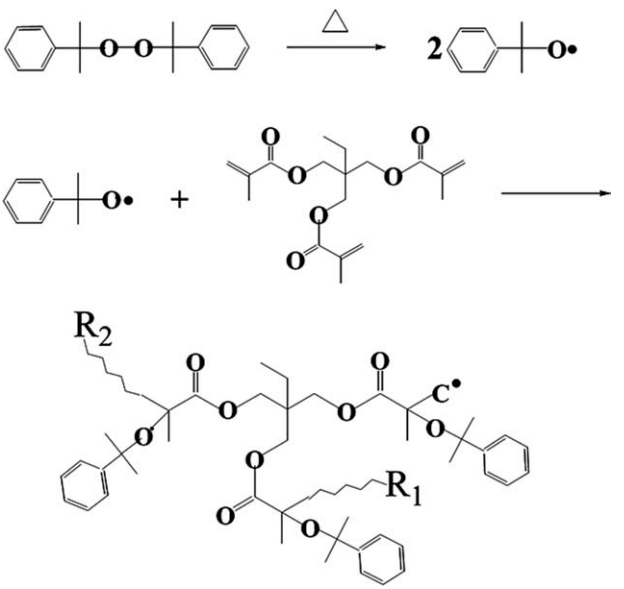

Figure 4 The schematic reaction of TMPTMA monomers.

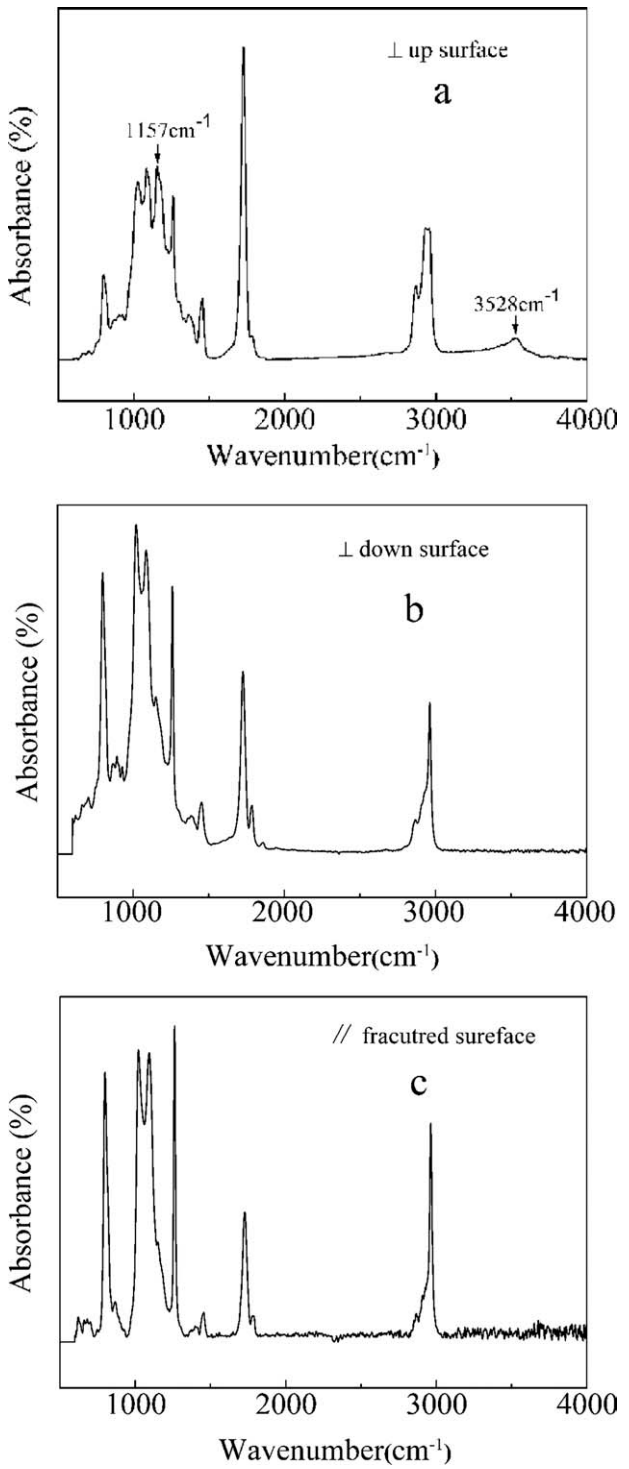

Figure 5 FTIR spectra of the different dispositions in AC-treated CER/TMPTMA system: ⊥, up surface (a); ⊥, down surface (b); and //, fractured surface (c).

In addition, it is generally thought that large amount of microgel particles would occur in certain sections at the beginning of the curing reactions of the thermoset systems. As curing reaction proceeds, the sizes of these microgel particles gradually become larger until the gelation takes place. Before gelation occurs, these microgel particles can be regarded as spherical dielectric. Under the action of the sufficiently high electric fields, it should be possible to deform spherical microdomains into ellipsoids and, for a liquid system in which there are many charged microgel particles formed during cure, the ellipsoids can be sufficiently stretched such that they interconnect to form lamellae that penetrate through the samples.[27] Thus, by using an amorphous structure to a well-regulated structure transition, a simple route to achieve highly ordered arrays of nanoscopic lamellae domains may be possible.

It can be easily expected that the external electric field may "purify" the cured epoxy systems: under the actions of the dielectrophoresis and electrophoresis as a result of the external electric field, free ions, voids, and other polar molecules can migrate toward two corresponding electrodes, respectively, according to whether the sign of the charge amount is positive or negative.

Figure 5 gives the comparison of FTIR results measured on the different positions of the cured CER/TMPTMA system along its thickness, that is, on the front (⊥, up surface) and rear (⊥, down surface) surfaces of the sample and on the middle position (//, fractured surface) of the sample thickness.

Of interest is that the IR absorption behaviors on these three positions are obviously distinguished from one another. As shown in Figure 5(a), the differences of IR absorption intensity values at the bands centered at 3528 and 1157 cm^{-1} are characteristic of —OH group and low molecules of anhydride, respectively; however, these peaks cannot be found at the sample surface [the bottom of the sample in Fig. 5(b)] contacted with the earth-grounded electrode and at the middle position of the sample thickness [Fig. 5(c)], revealing that the impurities move in the direction of two opposite electrodes under the action of the electric field applied. Especially, from the fact that the metal mold used is ground-earthed, it can be considered that the free ions and other charged particles arrived at the surface of the metal mold by the action of the electric field may be electrically neutralized, which may be the main reason why the characteristic IR absorption peaks cannot be observed at the sample surface ever contacted with the metal mold during the curing process.

Morphological characterization

Shown in Figure 6 are the AFM topographic and phase contrast images obtained in the cured CER and CER/TMPTMA systems with and without external electric field treatment during the curing process. The left and right images are the topography and phase contrast images, respectively.

It should be noted that the effect of the electric field treatment on the microstructures are more

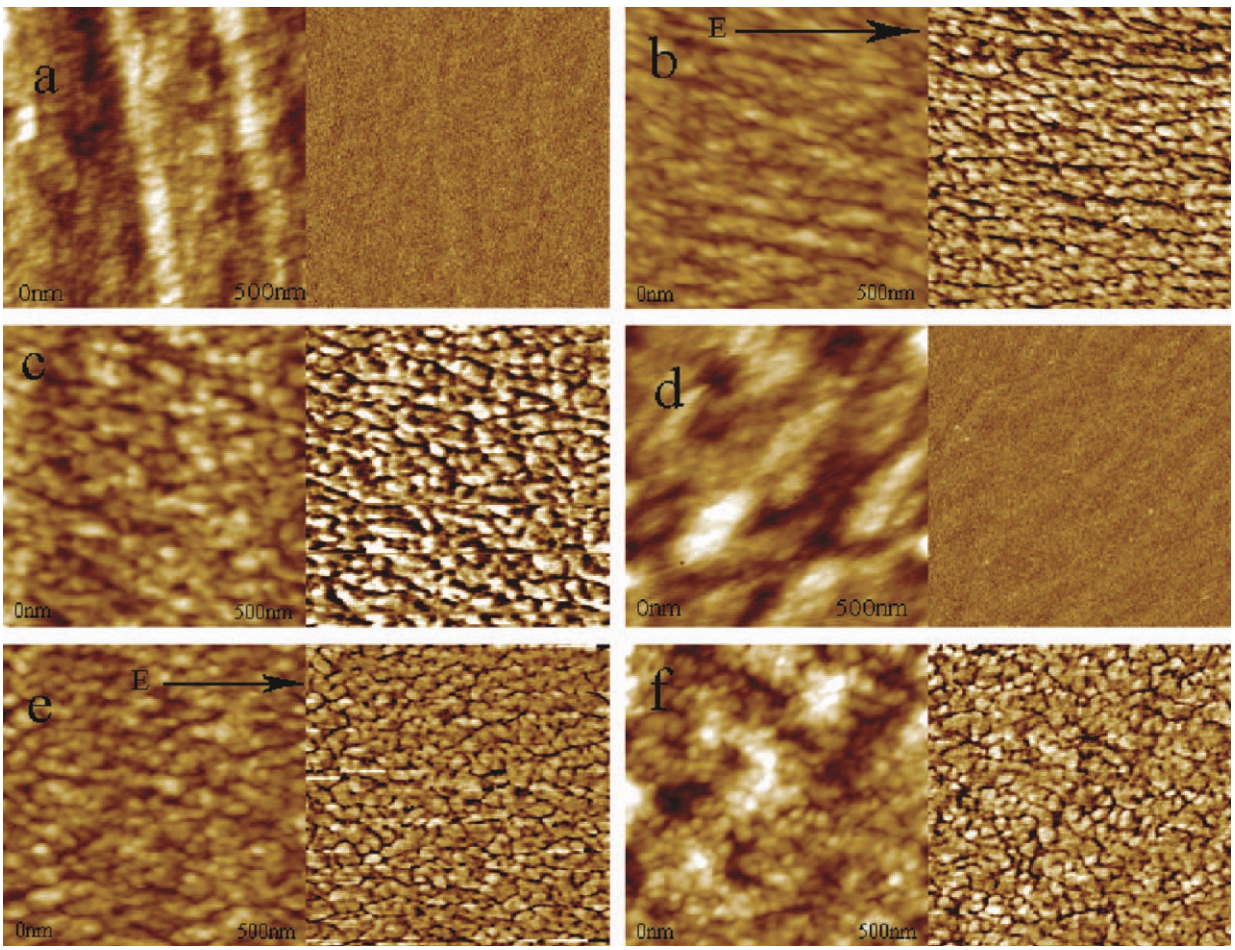

Figure 6 AFM images of nontreated CER system (a); treated CER system with // electric field (b); treated CER system with ⊥ electric field (c); nontreated CER/TMPTMA system (d); treated CER/TMPTMA system with // electric field (e); and treated CER/TMPTMA system with ⊥ electric field (f). [Color figure can be viewed in the online issue, which is available at wileyonlinelibrary.com.]

conspicuous: for the systems cured without the external electric field treatment, the homogeneous microstructures are observed as shown in Figure 6(a,d), which may depict the developed cross-linked networks of the CER and CER/TMPTMA systems; when the external electric field are applied during the curing reaction of the CER and CER/TMPTMA systems, the apparent changes in the microstructures become visible, that is, the resulting anhydride-CER and CER/TMPTMA systems newly display the nanostructured two-phase morphologies (e.g., nodular structures) along the directions of both parallel and perpendicular to the external electric field applied. The dark regions may be assigned to the "softer" nature compared with the nodules with higher cross-link densities. Moreover, there are apparent differences between the microstructures of the CER and CER/TMPTMA systems.

The phase contrast image reveals the presence of oval black domains that may be related to the softer phase, that is, the lower cross-linking density phase. These domains have the typical sizes of 40 and 20 nm along the longer and shorter axis, respectively. The lower phase contrast region is observed to occupy approximately 90% of the total surface area. These contours can be related to the rigid epoxy phase, the cross-linking density of which is relatively higher than that of the black domains regions.

By comparing two phase contrast images in Figure 6(b,c) or (d,e), one can affirm that the black domains in the AFM images for the cured anhydride-CER and CER/TMPTMA systems really correspond to the "soft" phase which, has the relatively lower cross-linking density, and confirm the presence of the higher cross-linking density domains where nanoparticles are dispersed over the sample volume and they are found to further elongate in the direction parallel to the external electrical field applied to the epoxy systems under the curing process.

Additionally, it is noteworthy that for the cured CER and CER/TMPTMA systems, the topography images corresponding to the directions perpendicular and parallel to the external electric field differ considerably from each other.

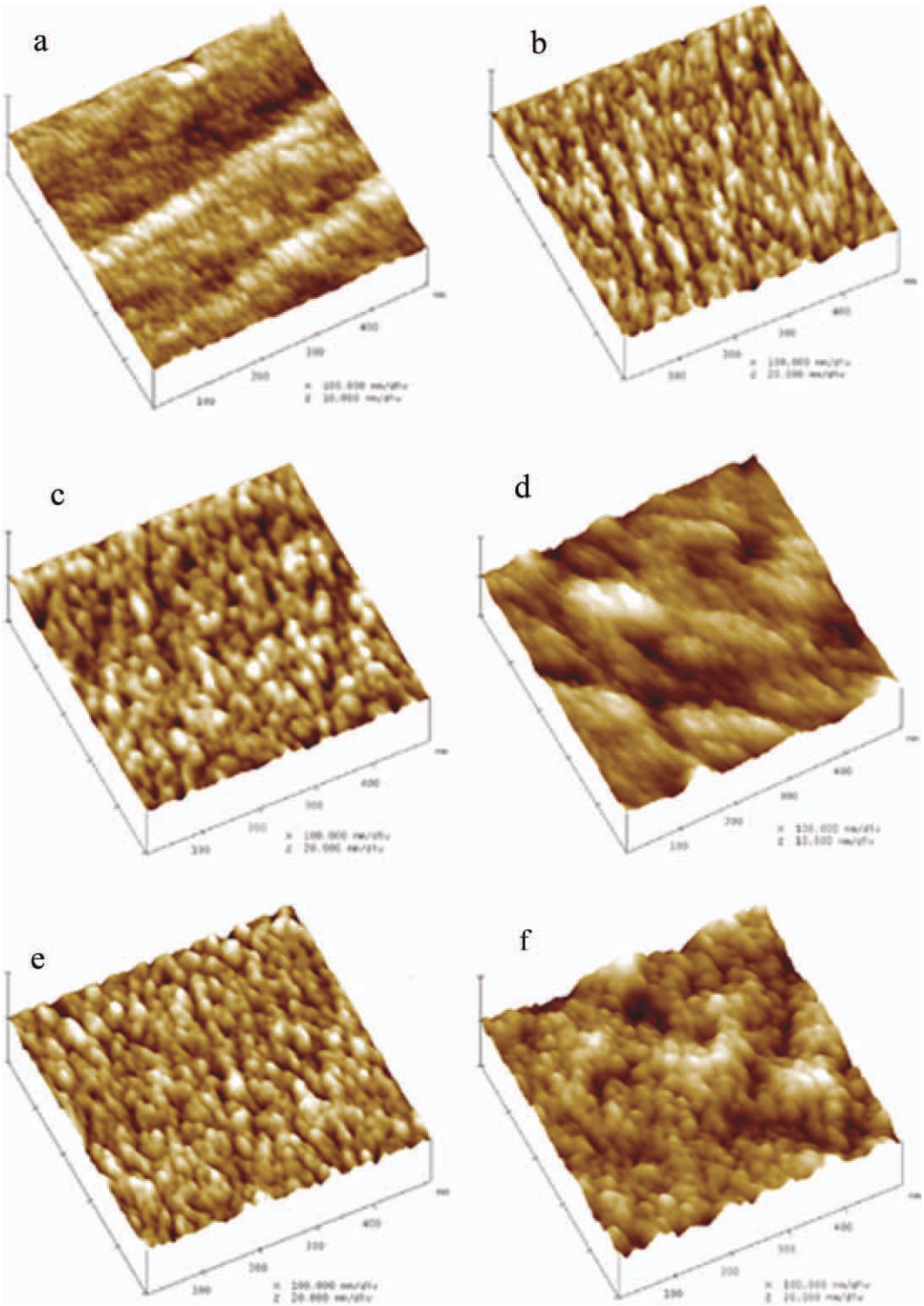

Figure 7 AFM topography images of nontreated CER system (a); treated CER system with // electric field (b); treated CER system with ⊥ electric field (c); nontreated CER/TMPTMA system (d); treated CER/TMPTMA system with // electric field (e); and treated CER/TMPTMA system with ⊥ electric field (f). [Color figure can be viewed in the online issue, which is available at wileyonlinelibrary.com.]

Figure 7 gives the AFM topography images of the different cured epoxy systems. As shown in Figure 7, the topography images of the CER and CER/TMPTMA systems cured without any aid of the electric field are characterized by much lower roughness and rather homogeneous surface, and the surface roughness of these two systems remains almost the same as shown in Figure 7(a,d). Whereas after they

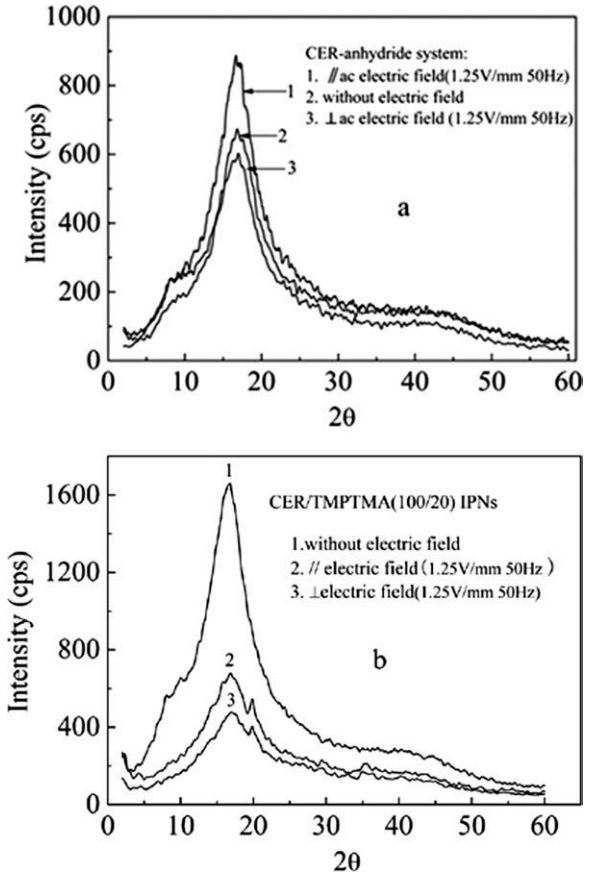

Figure 8 Wide-angle X-ray diffraction profiles of CER (a) and CER/TMPTMA (100/20) IPNs (b) with or without the aid of electric field (1250 V/mm, 50 Hz) during the curing process.

are subjected to the external electric fields during curing process, their topography images display remarkable changes: (i) in comparison with the cured systems without any electric field treatment, the topography images for the cured samples with treatment become more rugged in the directions both parallel and perpendicular to the direction of electric field as shown in Figure 7(b,c,e,f); (ii) for the systems cured with the aid of the external electric field, the topography images along the direction perpendicular to the external electric field is different from those parallel to the external electric field. Although the topography images along the direction parallel to the electric field also display rugged structure, they show relatively more regular structure in contrast with those along the direction perpendicular to the electric field [Fig. 7(b,e)], which reveals that external electric field treatment during the curing reaction for the CER and CER/TMPTMA systems has an important effect on the modification of their microstructures.

The microstructure changes in the directions both parallel and perpendicular to the direction of electric field in the CER and CER/TMPTMA systems also are confirmed by wide-angle X-ray diffraction profiles as shown in Figure 8.

The knowledge of the curing reaction process of the epoxy systems under the action of the applied electric field is helpful to understand the mechanism of the formation of the nanostructures in the CER and CER/TMPTMA systems. The formation of the microstructures in the CER and CER/TMPTMA systems can be schematically illustrated as depicted in Figure 9.

In the absence of the action of the external electric field, the molecules containing the permanent dipoles are in disorder dispersion in the uncured systems as shown in Figure 9(a) (the curve shapes between two plate electrodes stand for the molecules containing the permanent dipoles), whereas in the presence of the electric field between two plate electrodes, these molecules containing the permanent dipoles can display time-varying fluctuations with the changes of the applied electric field before the beginning of the curing reaction [Fig. 9(b)]. As the curing reaction proceeds, the particles in microgel state begin to appear as nucleation centers in the system as shown in Figure 9(c)[21] (the black dots between two plate electrodes stand for the microgel particles). The types of response of these microgel particles on the external electric field are rotation, deformation, orientation, and alignment along the direction of electric field, respectively, in the liquid medium as shown in Figure 9(d) (the irregular rods between two plate electrodes stand for the microgel particles, which have been rotated, deformed, and aligned along the direction of electric field).

According to Figures 3 and 4, before the gelation occurs in the systems, the microgel particles can be regarded as "active microgel particles" owing to their reactivity. With the aid of the applied electric field, these active microgel particles have to be deformable (nonrigid) in the liquid medium

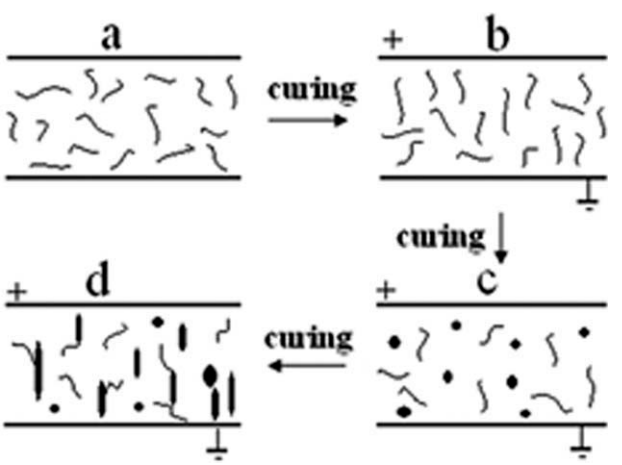

Figure 9 Formation of microstructures in the CER and CER/TMPTMA systems.

[Fig. 9(d)], leading to the transformation into asymmetric dielectric spheres, that is, ellipsoids. The electric field inside these asymmetry spheres is nonuniform and can be calculated by using depolarization factor for ellipsoid. Considering an ellipsoid has the axes a, b, and c aligned with the x, y, and z axes, respectively, according to Stratton,[28] and is immersed in a dielectric medium, its dipole moment is defined as:

$$\mu_a = A\frac{E_a(\varepsilon_p - \varepsilon_c)}{1+\beta n_a},\ \mu_b = A\frac{E_b(\varepsilon_p - \varepsilon_c)}{1+\beta n_b},\ \mu_c = A\frac{E_c(\varepsilon_p - \varepsilon_c)}{1+\beta n_c}$$
$$A = 4\pi abc/3,\quad \beta = (\varepsilon_p - \varepsilon_c)/\varepsilon_c \quad (1)$$

where μ_a, μ_b, and μ_c are the dipole moments along the directions of axes of a, b, and c, respectively; ε_p and ε_c are dielectric permittivities of an ellipsoid and a dielectric medium, respectively; E_a, E_b, and E_c are the electric field intensities along the axes of a, b, and c, respectively; and n_a, n_b, and n_c are the depolarization factors along the axes of a, b, and c, respectively.

From eq. (1), the value of ε_c is variable in the different curing stages. Thus, the dipole moment of a microgel particle is also changeable. In the presence of electric field, the microgel particles with different dipole moments along the axes of a, b, and c can be orientated, and the response of the longest axis of the particle on the orientation angle displays asymmetric distribution. These may lead to the formation of the microstructures in the cured anhydride-CER and CER/TMPTMA systems as shown in Figures 6 and 7. In addition, it is thought that the nanoellipsoid microstructure in the CER/TMPTMA system is closely related to the formation of sequential IPNs, and the nanolamellae microstructure existing in the CER system may be ascribed to the "dynamic curing reaction" between microgel particles and/or oligomers continuously under the action of AC electric field.

Changes in physical properties

It is well known that the macroscopic physical properties of organic materials, such as polymers and molecular aggregates, strongly depend on their microscopic structures. The polymers in which the minor phases are oriented or aligned in a desired direction should demonstrate unique electrical, optical, and mechanical properties.

Thermal property

The CER and CER/TMPTMA systems with and without the applied electric field treatment were subjected to the dynamic mechanical analysis. Figure 10 shows the variation in mechanical tan δ.

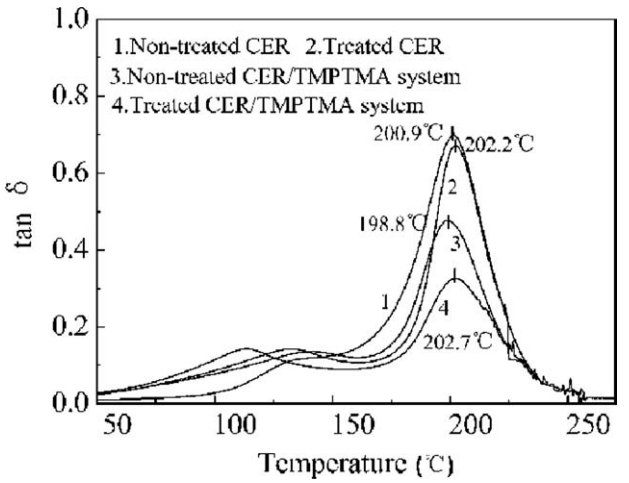

Figure 10 Dynamic mechanical analysis spectra as a function of temperature for the cured CER and CER/TMPTMA epoxy systems with and without the electric field treatment.

From Figure 10, it is clear that there is a similar tendency in tan δ between the aligned and the unaligned networks in the CER system as well as the CER/TMPTMA system. A relatively strong low-temperature relaxation peak (l-T_g), which is clearly separated from the high-temperature relaxation peak (h-T_g) centering at 198°C and 203°C is observed between 100°C and 150°C. In addition, an obvious difference is that the h-T_g values of the systems cured with the aid of the applied electric field further shift toward the high temperature compared with those cured in the absence of the applied electric field, whereas the l-T_g values shift toward low temperature, which reveals that the applied electric field shows the significant effects on the cross-linking networks of the CER and CER/TMPTMA systems during the curing reaction. It can be considered that the existence of two relaxation peaks in the resulting systems studied may be attributed to the isothermal curing condition, which leads to the formation of the defective structures in the systems. The high- and low-temperature relaxation peaks should be assigned to the higher and lower cross-linking density phases, respectively. However, the shift in the T_g value implies a "very high degree of structural heterogeneity" in the systems subjected to the applied electric fields. This is in good agreement with the results observed in AFM images in Figures 6 and 7.

It is also thought that the alignment taking place during curing influences the cross-linking structure of polymer. The lower cross-linking density regions of aligned polymers [the dark regions in Fig. 6(b,c,e,f)] indicates that there exists less intermolecular interaction, which may explain the shift of

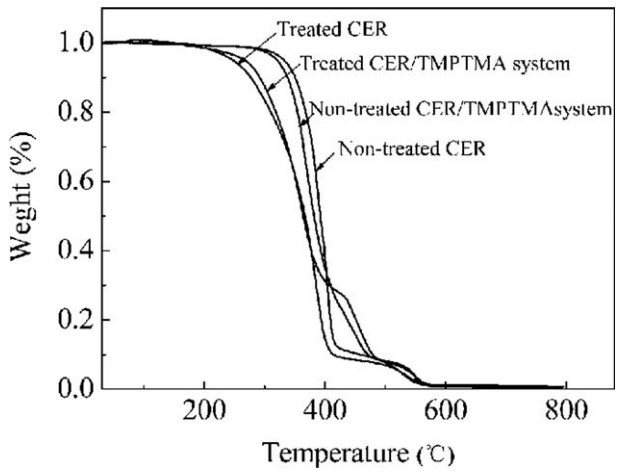

Figure 11 TGA curves of the different systems as a function of temperature.

l-T_g values observed in the dynamic mechanical thermal analysis measurement. The lamellae and nodular structures induced by the external electric field seem to display much stronger rigidity than that found in the systems cured without the external electric field (Fig. 6), revealing the enhancement of cross-linking density in these regions, which results in the shift of h-T_g values. The enhancements of the glass-transition temperature and the cross-linking density in polymers aligned or orientated by the external field have been found in some literatures.[29]

To understand the influence of the external electric fields on the thermal stability of the cured systems, TGA measurement is carried out. Results from TGA measurement are shown in Figure 11. From Figure 11, it is very clear that in contrast with the resulting anhydride-CER and CER/TMPTMA systems in the absence of the applied electric fields, the thermal stability of the systems in presence of the applied electric fields becomes deteriorated. It is thought that the thermal stability of the cured systems is strongly associated with their network structures. From the results of AFM and dynamic mechanical thermal analysis measurements, we have confirmed that despite the existence of high cross-linking domains, the structure obtained after alignment contains a large number of defects, e.g., some low cross-linking domains occur in the whole cross-linking networks of the cured systems with being subjected to the applied electric fields. The low cross-linking domains are approximately 10% of the total surface area, which may cause reduction in the thermal stability.

Dielectric measurements

From the above-mentioned experimental results, it can be expected that the curing systems studied here, which have been cured under the action of various kinds of external electric field, may display their own unique dielectric properties.

Figures 12 and 13 show the dependences of dielectric permittivity and loss tangent on the frequency in the range of 100 Hz to 10 MHz for the cured CER and CER/TMPTMA systems, respectively.

As can be seen in Figure 12, the dielectric permittivity seems to be a little lower for the cured CER system with the electric field treatment than for that without any treatment, whereas the dielectric loss tangent is nearly the same for two cases. The decrease in the dielectric permittivity is likely attributed to the increase in the degree of the cross-linking by the aid of the electric field treatment.

As well known, the dielectric permittivity can be expressed as

$$\varepsilon = 1 + \frac{\sum_{i=1}^{N} q_i l_i}{\varepsilon_0 V E} \tag{2}$$

where N is the total number of the dipoles; V is the volume; E is the electric field; ε_0 is the permittivity

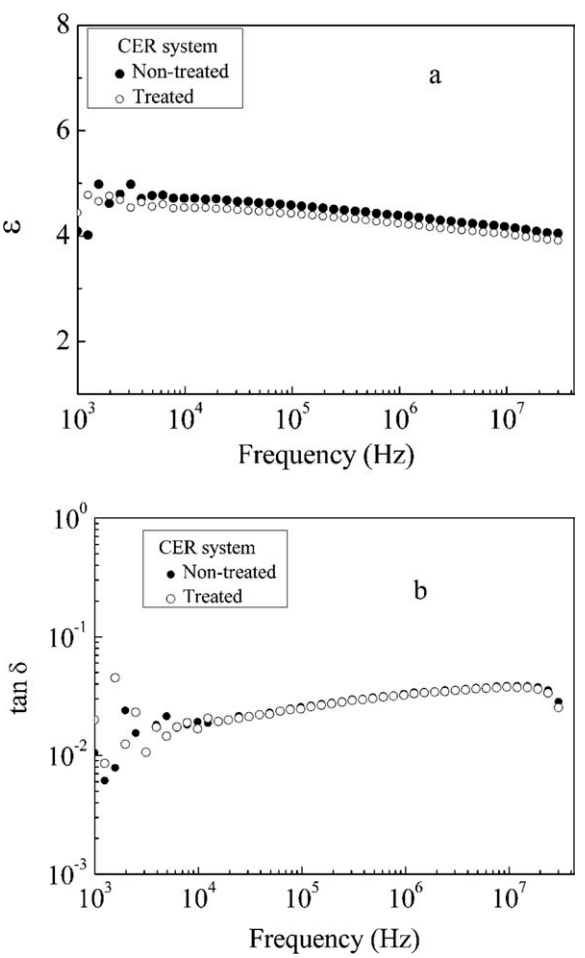

Figure 12 Dependences of dielectric permittivity (a) and loss tangent (b) for the cured CER systems with and without the aid of the external electric field.

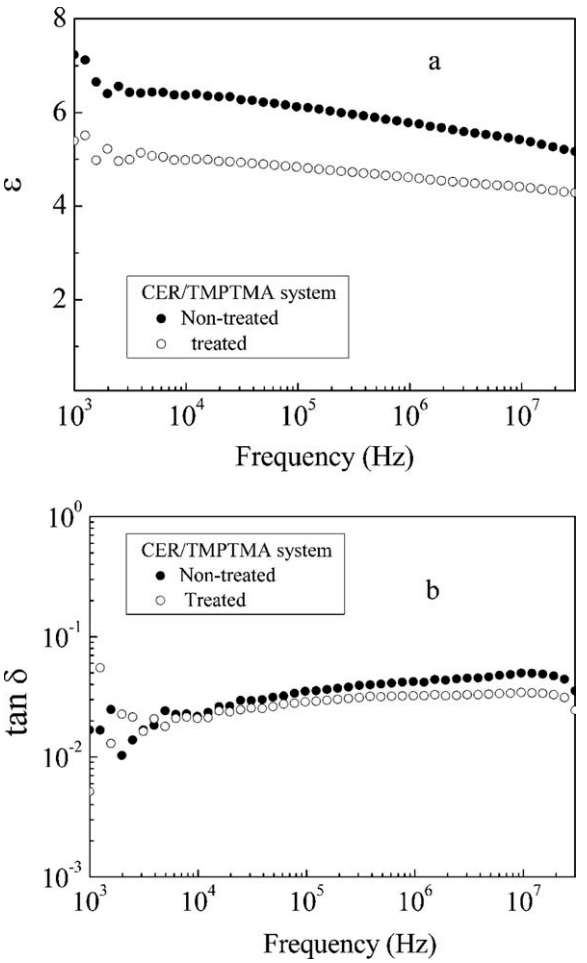

Figure 13 Dependences of dielectric permittivity (a) and loss tangent (b) for the cured CER/TMPTMA system with and without the aid of the external electric field.

of vacuum; and q_i and l_i are the electric charge and the effective length of an arbitrary dipole in a dielectric, respectively.

As can be easily expected, the only variable parameter in eq. (2) is the effective length of a dipole, provided that the dielectric material system is not changed in its composition. In the other hand, the effective length of a dipole can be considered to vary, depending on the degree of the motion of the dipole, that is, the molecular motion. The higher the degree of the cross-linking for a cured epoxy system, the more difficult the motion of the molecules, leading to the reduction of the effective length values of the dipoles and, as a result, the decrease in the dielectric permittivity and loss tangent.

Compared with the neat CER system, the differences of the dielectric properties are so obvious between the cured CER/TMPTMA systems with and without the electric field treatment as shown in Figure 13: the electric field treatment leads to significant reduction in both the dielectric permittivity and loss tangent of the cured CER/TMPTMA systems.

As mentioned above, two sequential cross-linking reactions can occur during the curing process of a CER/TMPTMA system, and the cross-linking network of TMPTMA likely gives an obstacle to the formation of the CER cross-linking network, which may cause a decrease in the total density of the cross-linking for the cured epoxy system considered.

Also, it may be rather difficult for CER and TMPTMA in the liquid state to be mixed with each other to form a completely homogeneous dispersion system because of their high values of viscosity, although great attention is paid to the mixing process.

In the case of the multicomponent medium like the CER/TMPTMA system investigated, the poorer the dispersion of the individual component, the larger the effective contact area between the components with different dielectric properties, resulting in the increase in the interfacial polarization, which can be also one of the main reasons why the electric field treatment effect is more significant for the

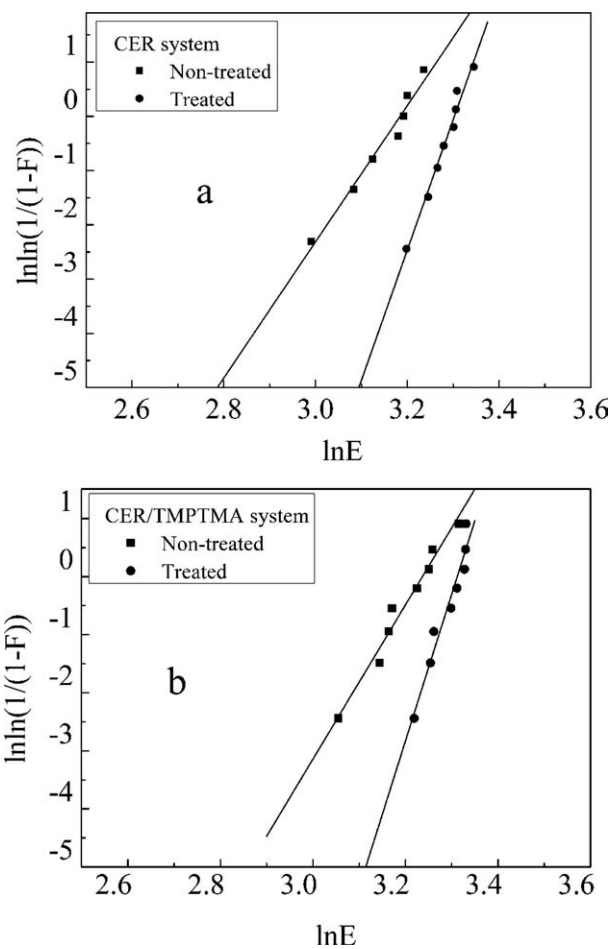

Figure 14 Weibull plots for the cumulative breakdown strength characteristics of CER system (a) and CER/TMPTMA system (b).

TABLE II
Characteristic Breakdown Increment after the Electric Field Treatment

Sample	E_S (kV/mm) Before	E_S (kV/mm) After	ΔE_S (%)
The CER system	24.03	27.16	13
The CER/TMPTMA system	25.41	28.10	11

cured the CER/TMPTMA system than for the cured CER system.

The dielectric measurement results are in good agreement with the above-considered data of the physicochemical and thermomechanical analyses, which suggests that the external electric field applied to the CER/TMPTMA system under curing may play an important role in further improving the dispersion of the TMPTMA into the CER region and also accelerate the curing reaction of CER, so that the density of the cross-linking network for the cured CER/TMPTMA system can be much denser compared with that for the system without any aid of the external electric field.

Weibull statistical analysis has been widely used in determining the dielectric breakdown characteristics of the dielectric and insulating materials.[30,31] Figure 14 gives the results of Weibull statistical analysis on the dielectric breakdown characteristics of the cured CER and CER/TMPTMA systems, respectively. The values of the Weibull shape parameter β are 24.01 and 12.55 for CER cured with and without the aid of the electric field, respectively, whereas they are 25.29 and 13.3 for CER/TMPTMA cured with and without the aid of the electric field, respectively. An increase in the shape parameters β (a decrease in the scatter) means that the structure of the epoxy system cured under the action of electric field is more homogeneous than that of the system cured without any aid of the external electric field. This may be attributed to the "purification" of the curing systems caused by the external electric field as depicted in Figure 5.

As can be seen from Figure 14 and Table II, the cured CER/TMPTMA system, in the absence of the electric field treatment, shows a little higher dielectric breakdown strength than the cured CER, that is, the introduction of TMPTMA into the conventional CER system does not give any negative influences on the dielectric breakdown characteristics of the resulting CER/TMPTMA system.

Of greater interest is that the dielectric breakdown strength is significantly increased by the aid of the external electric field during the curing reaction of the CER and CER/TMPTMA systems. This result can be also ascribed to the increase in the density of the cross-linking network and the reduction of defects in the networks by the electric field treatment.

CONCLUSIONS

In this article, the effects of the external electric field on the morphological and physical properties of the CER and its blend (CER/TMPTMA) were studied through the characterization by means of the physicochemical measurements, e.g., dynamic mechanical analysis, FTIR, dielectric spectroscopy, and AFM observation.

The experiment results clearly show that alignment of the apparent spherical micelles whose size are roughly tenth of nanometer can be observed in the resulting anhydride-CER system and IPNs system subjected to the external electric field during their curing stages.

These microstructures obtained by the electric field treatment method can result in the modification of thermal and dielectric properties for the cured epoxy systems. The electric field treatment during the curing process of an epoxy system can increase significantly the dielectric breakdown strength of the cured epoxy insulation system and at the same time reduce its dielectric permittivity and loss without any additive economic investment, which is of great practical significance.

References

1. Kim, G. H.; Shkel, Y. M.; Rowlands, R. E. Proc SPIE 2003, 5051, 442.
2. Shkel, Y. M.; Kim, G. H.; Rowlands, R. E. Presented at the International Symposium on Experimental Mechanics, Taipei, Taiwan, 2002.
3. Kim, G. H. Field Aided Technology for Local Micro-Tailoring of Polymeric Composites with Multi-Functional Response. University of Wisconsin: Madison, WI, 2003.
4. Lee, K. F.; Villeneuve, D. M.; Corkum, P. B.; Sphapiro, E. A. Phys Rev Lett 2004, 93, 233601.
5. Larsen, J. J.; Laesen, I. W.; Stapelfelt, H. Phys Rev Lett 1999, 83, 1123.
6. Jurjiu, A.; Friedrich, C.; Blumen, A. Chem Phys 2002, 284, 221.
7. Chen, Z. R.; Kornfied, J. A. Polymer 1998, 39, 4679.
8. Albalak, R. J.; Thomas, E. L. J Polym Sci Part B: Polym Phys 1993, 31, 37.
9. Tammer, M.; Li, J.; Komp, A.; Finkelmann, H.; et al. Macromol Chem Phys 2005, 206, 709.
10. Urayama, K.; Honda, S.; Tahigawa, T. Macromolecules 2006, 39, 1943.
11. Al-Halk, M. S.; Garmestani, H.; Li, D. S.; Hussaini, M. Y.; Sablin, S.; Tannenbaum, R.; Dahmen, K. J Polym Sci Part B: Polym Phys 2004, 42, 1586.
12. Harada, M.; Ochi, M.; Tobita, M.; Kimura, T.; Ishigaki, T.; Shimoyama, N.; Aoki, H. J Polym Sci Part B: Polym Phys 2004, 42, 758.
13. Boker, A.; Elbs, H.; Hansel, H.; Knoll, A.; Ludwigs, S.; Zettl, H.; Zvelindovsky, A. V.; Svink, G. F. A.; Urban, V.; Abetz, V.; Miiller, A. H. E; Krausch, G. Macromolecules 2003, 36, 8078.

14. Albrecht, I. T.; Schotter, J.; Kastle, C. A.; Emley, N.; Shibauchi, M. T.; Russell, T. P. Science 2000, 290, 2126.
15. Martin, C. A.; Sandler, J. K. W.; Windle, A. H.; Schwarz, M. K.; Auhofer, W. B.; Schulte, K.; Shaffer, M. S. P. Polymer 2005, 46, 877.
16. Khastgir, D.; Adachi, K. J Polym Sci Part B: Polym Phys 1999, 37, 3065.
17. Khastgir, D.; Adachi, K. Polymer 2000, 41, 6403.
18. Voicu, N. E.; Harkema, S.; Steiner, U. Adv Funct Mater 2006, 16, 926.
19. Onuki, A.; Fukuda, J. Macromolecules 1995, 28, 8788.
20. Xu, T.; Zvelindovsky, A. V.; Sevink, G. J. A. Macromolecules 2004, 37, 6980.
21. Amundson, K.; Helfand, E.; Davis, D. D.; Quan, X.; Smith, S. D. Macromolecules 1991, 24, 6546.
22. Thurn-Albrecht, T.; DeRouchey, J.; Russell, T. P.; Jaeger, H. M. Macromolecules 2000, 33, 3250.
23. Amundson, K.; Helfand, E.; Quan, X.; Smith, S. D. Macromolecules 1993, 26, 2698.
24. Cheng, J.; Wang, S. Presented at the 6th International Conference on Properties and Applications of Dielectric Materials, Xi'an, China, June 21–26, 2000.
25. Zhang, Z.; Wong, C. P. J Appl Polym Sci 2002, 86, 1572.
26. Smith, J. D. B. J Appl Polym Sci 1981, 26, 979.
27. Landau, L. D.; Lifshitz, E. M. Electrodynamics of Continuous Media; Pergamon: Oxford, 1960; Chapter II.
28. Stratton, J. A. Electromagnetic Theory; McGraw-Hill: New York, 1941.
29. Gerzeski, R. H. In Proceedings of the 19th SAMPE Technical Conference, Covina, CA, 1989; p 1913.
30. Fabiani, D.; Simoni, L. IEEE Trans Dielectric Electric Insulat 2005, 12, 11.
31. Irurzun, I. M.; Vicente, J. L.; Cordero, M. C.; Mola, E. E. Phys Rev E 2000, 63, 016110.